Immunobiology 224 (2019) 80–93

Contents lists available at ScienceDirect

Immunobiology

journal homepage: www.elsevier.com/locate/imbio

Activation of human macrophage sodium channels regulates RNA processing to increase expression of the DNA repair protein PPP1R10

Chelsea R. White[a], Matthew Dungan[a], Michael D. Carrithers[a,b,c,*]

[a] Department of Neurology, University of Illinois College of Medicine, Chicago, IL 60612, United States
[b] Program in Neuroscience, University of Illinois College of Medicine, Chicago, IL 60612, United States
[c] Jesse Brown Veterans Affairs Medical Center, Chicago, IL 60612, United States

ARTICLE INFO

Keywords:
Innate immune signaling
DNA repair
SCN5A
SCN10A
PPP1R10

ABSTRACT

Prior work demonstrated that a splice variant of *SCN5A*, a voltage-gated sodium channel gene, acts as a cytoplasmic sensor for viral dsRNA in human macrophages. Expression of this channel also polarizes macrophages to an anti-inflammatory phenotype in vitro and in vivo. Here we utilized global expression analysis of splice variants to identify novel channel-dependent signaling mechanisms. Pharmacological activation of voltage-gated sodium channels in human macrophages, but not treatment with cytoplasmic poly I:C, was associated with splicing of a retained intron in transcripts of *PPP1R10*, a regulator of phosphatase activity and DNA repair. Microarray analysis also demonstrated expression of a novel sodium channel splice variant, human macrophage *SCN10A*, that contains a similar exon deletion as *SCN5A*. *SCN10A* localizes to cytoplasmic and nuclear vesicles in human macrophages. Simultaneous expression of human macrophage *SCN5A* and *SCN10A* was required to decrease expression of the retained intron and increase protein expression of *PPP1R10*. Channel activation also increased protein expression of the splicing factor *EFTUD2*, and knockdown of *EFTUD2* prevented channel dependent splicing of the retained *PPP1R10* intron. Knockdown of the *SCN5A* and *SCN10A* variants in human macrophages reduced the severity of dsDNA breaks induced by treatment with bleomycin and type 1 interferon. These results suggested that human macrophage *SCN5A* and *SCN10A* variants mediate an innate immune signaling pathway that limits DNA damage through increased expression of *PPP1R10*. The functional significance of this pathway is that it may prevent cytotoxicity during inflammatory responses.

1. Introduction

Macrophages respond to infection and injury through pattern recognition signaling pathways that link ligand-mediated receptor activation to downstream regulation of transcription. Pathogen and danger-associated molecular patterns that activate pattern recognition receptors include extracellular ligands such as lipopolysaccharide (Poltorak et al., 1998), cytosolic viral dsRNA (Yoneyama et al., 2004), and cytosolic dsDNA (Ishikawa et al., 2009; Ablasser et al., 2013) generated by intracellular infection or endogenous mechanisms of cellular injury. These signaling mechanisms initiate acute immune responses but are also associated with genetic susceptibility to severe forms of chronic inflammatory disease (Li et al., 2017; Rice et al., 2013).

Prior work from this laboratory demonstrated that intracellular variants of voltage-gated sodium channels act as pattern recognition molecules for viral-associated molecular patterns (Jones et al., 2014; Lee et al., 2015). One of these variants, human macrophage *SCN5A*, regulates a channel-dependent signaling pathway mediated by localized calcium flux and *ATF-2*, a cAMP-dependent transcription factor (Jones et al., 2014). Cytoplasmic dsRNA directly activates this channel to initiate signaling and increase transcription of anti-viral genes such as Type I interferons. This mechanism represents a distinct innate immune signaling pathway because it is not dependent on expression of Rig-like receptors such as RIG-I or downstream signaling components in the toll-like receptor pathways. An invertebrate variant of this channel that is activated by mimics of viral-derived ssRNA has also been identified. Voltage-gated sodium channel, *AAEL006019*, is expressed in *Aedes aegypti*, the yellow fever mosquito (Lee et al., 2015). Activation of this intracellular channel regulates transcription of mediators of insect

Abbreviations: ATF2, activating transcription factor 2; DAPI, 4′,6-diamidino-2-phenylindole; dsRNA, double stranded RNA; EFTUD2, elongation factor Tu GTP binding domain containing 2; H2AX, histone family member H2A; IFN, interferon; MDM, monocyte-derived macrophages; PPP1R10, protein phosphatase 1 regulatory subunit 10; SCN, voltage-gated sodium channel gene

* Corresponding author at: Department of Neurology, University of Illinois College of Medicine, Chicago, IL 60612, United States.
E-mail address: mcar1@uic.edu (M.D. Carrithers).

https://doi.org/10.1016/j.imbio.2018.10.005
Received 20 August 2018; Received in revised form 12 October 2018; Accepted 16 October 2018
Available online 24 October 2018

Table 1
Reduced expression of a retained intron of *PPP1R10* in human monocyte-derived macrophages following sodium channel activation with veratridine versus treatment with either vehicle control or cytoplasmic poly IC.

Gene	PSR/Junction ID	Splicing Index (linear) (Veratridine vs. Vehicle)	ANOVA p-value	FDR p-value	Splicing Event Estimate (Veratridine vs. Vehicle)
PPP1R10	PSR06016933.hg.1	−5.07	0.00003	0.036	Intron Retention Exon junction 15/16
Gene	PSR/Junction ID	Splicing Index (linear) (Veratridine vs. Poly IC)	ANOVA p-value	FDR p-value	Splicing Event Estimate (Veratridine vs. Poly IC)
PPP1R10	PSR06016933.hg.1	−4.21	0.000007	0.015	Intron Retention Exon junction 15/16

Array analysis performed on a minimum of 3 separate RNA preparations from different donors. Data were analyzed with Transcriptome Analysis Console software (Affymetrix). Splicing index is calculated following normalization of relative gene expression levels. (FDR: false detection rate).

Table 2
No significant changes were observed in global gene expression of *PPP1R10* or of specific exon regions in human monocyte-derived macrophages following sodium channel activation with veratridine versus treatment with either vehicle control or cytoplasmic poly IC.

Gene	Gene-fold Change	Exon	PSR/Junction ID	Splicing Index (linear) (Veratridine vs. Vehicle)	ANOVA p-value	FDR p-value
PPP1R10	−1.10					
PPP1R10		10	PSR06016950.hg.1	1.00	0.83	0.94
PPP1R10		11	PSR06016949.hg.1	1.05	0.64	0.83
Gene	Gene-fold Change	Exon	PSR/Junction ID	Splicing Index (linear) (Veratridine vs. Poly IC)	ANOVA p-value	FDR p-value
PPP1R10	1.28					
PPP1R10		10	PSR06016950.hg.1	1.00	0.79	0.92
PPP1R10		11	PSR06016949.hg.1	1.02	0.63	0.84

Array analysis performed on a minimum of 3 separate RNA preparations from different donors. Data were analyzed with Transcriptome Analysis Console software (Affymetrix). Splicing index is calculated following normalization of relative gene expression levels. (FDR: false detection rate).

Table 3
Identification of alternatively spliced transcripts of voltage-gated sodium channels in human monocyte-derived macrophages as compared to pooled samples from cardiac muscle and dorsal root ganglion.

Gene	PSR/Junction ID	Splicing Index (linear) (MDM vs. DRG-Heart)	ANOVA p-value	FDR p-value	Splicing Event Estimate (MDM vs. DRG-Heart)
SCN10A	PSR03022313.hg.1	−14.18	0.00018	0.001	Alternative Exon, exon 23
SCN5A	PSR03022267.hg.1	−8.49	$5E^{-07}$	$9E^{-06}$	Alternative Exon, exon 24

Array analysis performed on a minimum of 3 separate RNA preparations from different donors. Data were analyzed with Transcriptome Analysis Console software (Affymetrix). Splicing index calculated following normalization of relative gene expression levels. (FDR: false detection rate).

innate immunity, *RelA* and *Ago2*.

Evidence also exists that human macrophage *SCN5A* regulates phenotype of inflammatory disease in vivo. Macrophages that express the human macrophage *SCN5A* splice variant in a mouse transgenic model ($C57BL^{cfms-hSCN5}$) have an anti-inflammatory phenotype and promote clinical recovery in experimental autoimmune encephalomyelitis (EAE) (Rahgozar et al., 2013). Based on these results, we reasoned that channel signaling limits injury mediated by either viral or danger-associated molecular patterns. The working hypothesis is that human macrophage sodium channels regulate multiple signaling pathways that maintain anti-viral host defense but limit inflammatory injury.

Here we utilized a next generation global genomic approach to identify novel signaling mechanisms in human macrophages that link channel activation to regulation of splicing of retained introns in RNA transcripts. Pharmacological activation of human macrophage sodium channels with veratridine, a channel agonist, leads to reduced expression of a retained intron in transcripts of *PPP1R10*, a regulatory subunit of protein phosphatase 1 (PP1) and a mediator of DNA repair (Kim et al., 2003; Landsverk et al., 2010). This response requires co-expression of *SCN5A*, a newly discovered intracellular splice variant of *SCN10A*, and the splicing factor *EFTUD2* (Fabrizio et al., 1997). Reduced expression of either channel increases the severity of dsDNA breaks induced by type I interferon and bleomycin.

2. Materials and methods

2.1. Cells

Human $CD14^+$ peripheral blood monocytes were obtained from Hemacare and differentiated to macrophages in RPMI media supplemented with 10% fetal bovine serum (FBS), sodium pyruvate, non-essential amino acids, and mCSF (macrophage colony stimulating factor, 20 ng/ml) for 7–10 days. These monocyte-derived macrophages (MDM) were grown on collagen coated coverslips (BD Bioscience). For induction of DNA damage and dsDNA breaks, MDM were treated with bleomycin (bleocin, Millipore, 1 μg/ml) and universal Type I interferon (human IFN-alpha A/D; 100 U/ml) for 6 h.

2.2. Microarray analysis

Total RNA was prepared from human MDM using column purification (Qiagen RNeasy). RNA from human myocardium and dorsal root ganglia were obtained from Clontech Laboratories. Labeling, hybridization, and scanning were performed at the Gene Expression

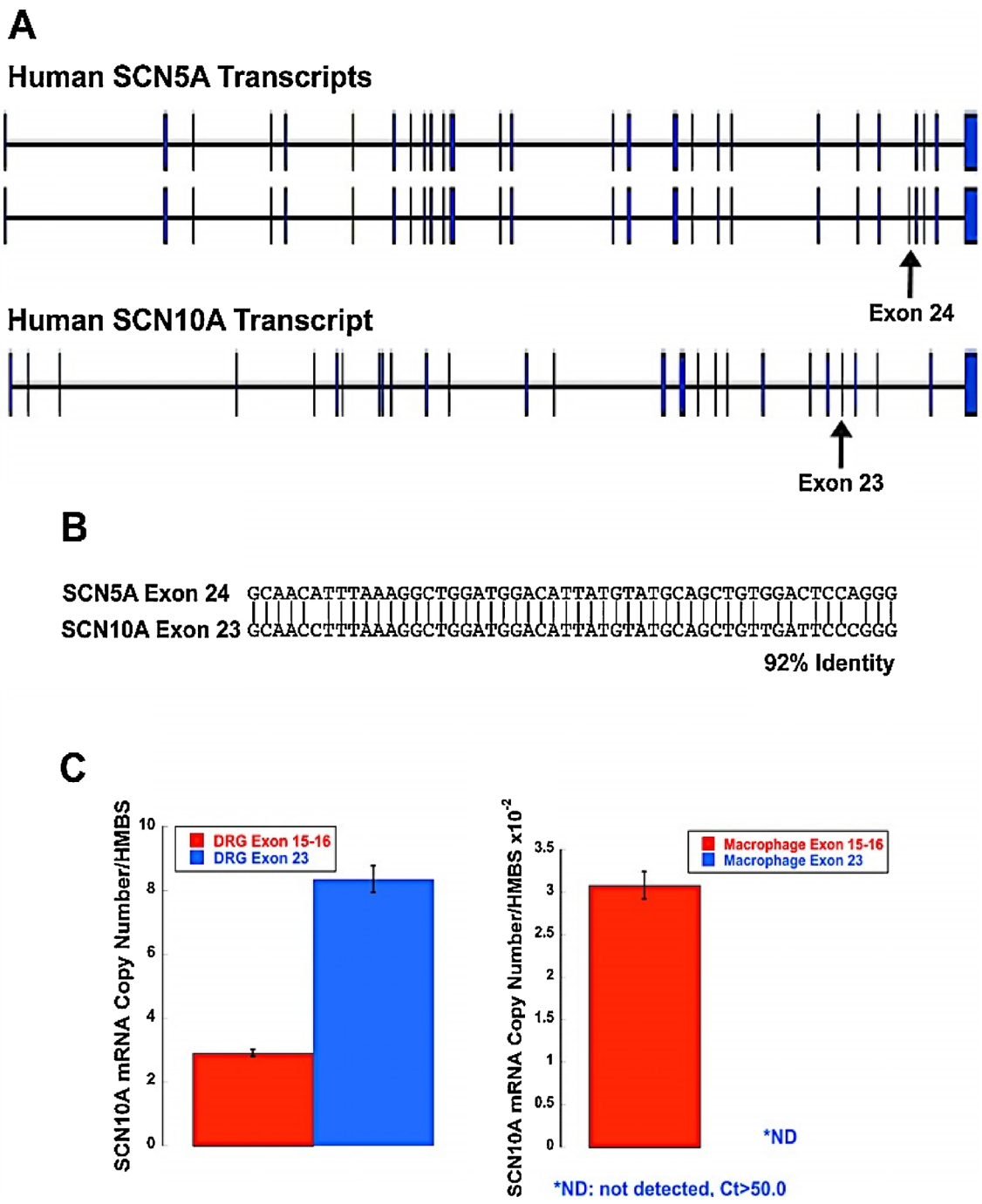

Fig. 1. Human macrophage *SCN10A* is a novel splice variant. As compared to transcripts from human heart and dorsal root ganglia (DRG), splicing analysis revealed expression of *SCN10A* transcripts in human MDM that contain an exon deletion that encodes for the extracellular selectivity filter (Table 3). (A) Both exon 23 in *SCN10A* and exon 24 in *SCN5A* encode a short amino acid sequence within the extracellular selectivity filter of the channels. These deletions in human macrophage variants alter the peak currents and ion selectivity of the channels so that they function as voltage-gated monovalent cation channels (Jones et al., 2014). (B) Pairwise alignment of the nucleotide sequences of exon 23 in *SCN10A* and exon 24 in *SCN5A* revealed 92% identity with an E value of $6e^{-20}$. This region encodes a 17 amino acid region that contains the extracellular selectivity filter and a portion of the ion pore. (C) The predicted alternative splicing of *SCN10A* was confirmed by quantitative PCR in human MDM. DRG and MDM express *SCN10A* transcripts that contain the common exons 15 and 16 (red). However, exon 23 was detected only in DRG samples and not in MDM (blue). For human DRG samples, *SCN10A* mRNA copies/(HMBS copy number) were 2.91 $\pm$ 0.11 and 8.36 $\pm$ 0.42, respectively for the common exon span (exons 15 and 16) and exon 23. For human MDM, *SCN10A* mRNA copies/(HMBS copy number x10^{-2}) were 3.08 $\pm$ 0.16 for the common exon span. *HMBS* (hydroxymethylbilane synthase) was utilized as the housekeeping gene for normalization between samples (n = 4 for each condition) (For interpretation of the references to colour in this figure legend, the reader is referred to the web version of this article).

Center at the University of Wisconsin Biotechnology Center (Madison, WI). Human Transcriptome Arrays (HTA 2.0, Affymetrix) were utilized. Data were analyzed using NetAffx software (Affymetrix). Fold change and *P*-values were based on at least 3 separate RNA preparations for each condition.

2.3. siRNA and Poly I:C transfection

Primary human MDM were transfected in serum-free Optimem media that contained 100 nM retinoic acid using the TransIT X2 transfection reagent (Mirus) and pooled ON-TARGETplus siRNA for

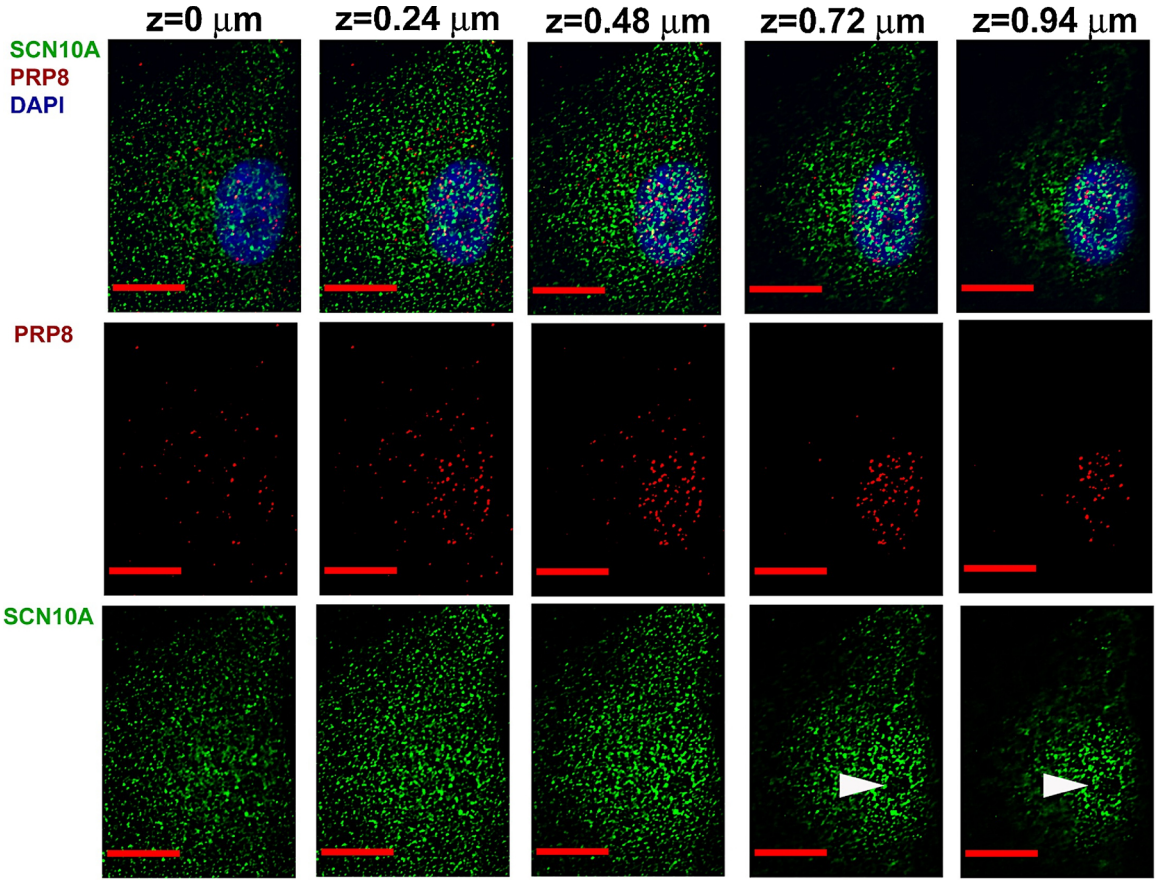

Fig. 2. *SCN10A* localizes to intracellular vesicles in the cytoplasm and nucleus of human macrophages. The subcellular localization of *SCN10A* human monocyte-derived macrophages was analyzed by immunofluorescence staining and deconvolution microscopy. As previously observed for the human macrophage *SCN5A* variant, *SCN10A* staining (green) demonstrated a vesicular appearance in the cytoplasm. However, a similar staining pattern was also observed in the nucleus (blue, DAPI stain). Staining for a nuclear protein, *PRP8* (red), is shown for comparison. Neither protein is identified in the nucleolus (white arrows). Scale bar, 10 μm. (For interpretation of the references to colour in this figure legend, the reader is referred to the web version of this article).

each target (Dharmacon). Cells were maintained in media with transfection complexes for 48 h prior to experiments. Knockdown was confirmed by quantitative real-time PCR and was greater than 75%.

Poly I:C (LMW; Invivogen) complexes were generated in Optimem using 10 μg/ml poly I:C and 30 μl of TransIT X2 transfection reagent/ml media (30 min at 25 °C). MDM were treated with 200 ng/ml poly I:C for 2 h.

2.4. Real time PCR

RNA purification, reverse transcription, quantitative real-time PCR (qPCR), and data analysis were performed as described previously (Jones et al., 2014; Carrithers et al., 2007). Data were acquired on a Cepheid SmartCycler and analyzed by the $2^{\Delta Ct}$ method with normalization to human *HMBS* (hydroxymethylbilane synthase). For the relative change in expression of the *PPP1R10* intron with pharmacological treatment, intron expression was normalized by the ΔC_t method to an upstream *PPP1R10* region that spans two exons (exons 10 and 11), and fold change between conditions was calculated by the $2^{\Delta\Delta Ct}$ method. The following TaqMan primers were obtained from Applied Biosystems/Life Technologies: Hs00609296 *(HMBS)*, Hs01045137 (*SCN10A*, spans exons 15/16), Hs01045146 (*SCN10A*, spans exons 22/23), Hs00160391 (*PPP1R10* spans exons 10/11), and custom assay AJBJXWN (*PPP1R10* intron at exon junction 15/16).

2.5. Immunofluorescence staining

For immunofluorescence staining, cell monlayers were fixed in 4% paraformaldehyde, washed with PBS, and blocked in PBS containing 2% serum, 0.1% Triton X-100, and 1% BSA. Primary and secondary antibodies were diluted in blocking solution. For primary antibody staining, rabbit anti-NaV1.8 (*SCN10A*) was from Alomone (ASC-016, 1:100 dilution); rabbit anti-EFTUD2 (1:1000 dilution), rabbit anti-53BP1 (1:200 dilution) and mouse anti-γH2AX (phospho S139, clone 9F3, 1:500 dilution) antibodies were from Abcam; mouse anti-PPP1R10 (PNUTS protein, clone F-8; 1:100 dilution) was from Santa Cruz Biotechnology (1:50 dilution); and isotype controls were from eBioscience. Alexa dye labeled secondary antibodies (donkey anti-mouse and anti-rabbit) were from Invitrogen. Treated cells were washed extensively with PBS prior to fixation and imaging.

2.6. Deconvolution fluorescence microscopy

Fluorescent images were acquired and analyzed using a Zeiss Axiovert 200 fluorescent microscope equipped with an Axiocam-MRm CCD camera (Zeiss) and a 63x objective (Zeiss Plan Apochromat, 1.4 oil). Multiple images in the Z-plane were acquired with 0.24 μm slices, and deconvolution was performed using Axiovision version 4.8 software.

2.7. D fluorescence difference gel electrophoresis (2D DIGE)

The cells were solubilized in 2-D cell lysis buffer (30 mM Tris – HCl, pH 8.8, containing 7 M urea, 2 M thiourea and 4% CHAPS). Protein concentration was measured using Bio-Rad protein assay method.

For each sample, 30 μg of protein was mixed with 1.0 μl of diluted

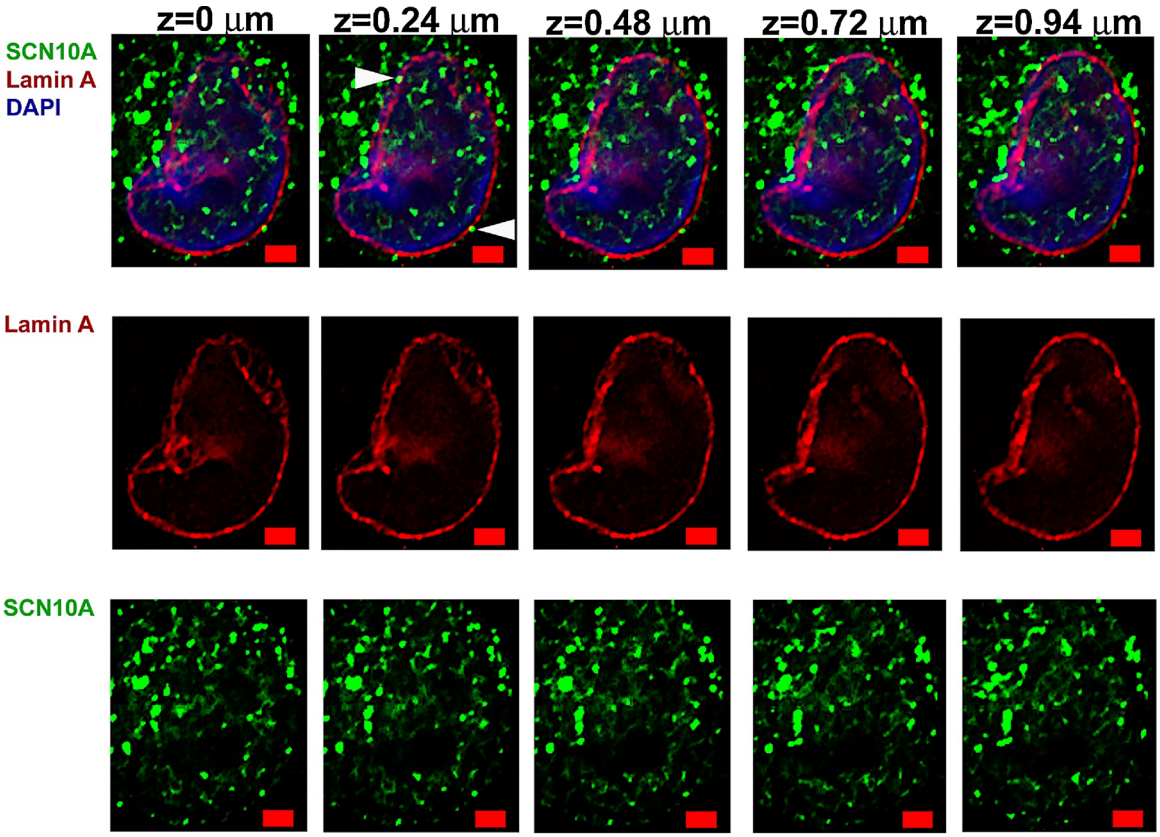

Fig. 3. *SCN10A* localizes to perinuclear, nuclear envelope, and intranuclear vesicles in human macrophages. The relative localization of *SCN10A* (green) and the nuclear envelope marker Lamin A (red) in human monocyte-derived macrophages was analyzed by immunofluorescence staining and deconvolution microscopy. A small number of *SCN10A*-positive vesicles appeared to localize to the nuclear envelope membrane (white arrows). However, most of the nuclear staining for *SCN10A* was intranuclear (DAPI, blue). Scale bar, 2 μm. (For interpretation of the references to colour in this figure legend, the reader is referred to the web version of this article).

CyDye, and kept in dark on ice for 30 min. Samples from each pair were labeled with Cy3 and Cy5 respectively. The labeling reaction was stopped by adding 1.0 μl of 10 mM lysine to each sample, and incubating in dark on ice for additional 15 min. The labeled samples were then mixed together. The 2 × 2-D Sample buffer (8 M urea, 4% CHAPS, 20 mg/ml DTT, 2% pharmalytes and trace amount of bromophenol blue), 100 μl Destreak solution and Rehydration buffer (7 M urea, 2 M thiourea, 4% CHAPS, 20 mg/ml DTT, 1% pharmalytes and trace amount of bromophenol blue) were added to the labeling mix to make the total volume of 250 μl. The labeled samples were mixed then loaded into a strip holder.

After loading the labeled samples, IEF (pH 3–10 Linear) was run following the protocol provided by GE Healthcare. Upon finishing the IEF, the IPG strips were incubated in the freshly made equilibration buffer-1 (50 mM Tris − HCl, pH 8.8, containing 6 M urea, 30% glycerol, 2% SDS, trace amount of bromophenol blue and 10 mg/ml DTT) for 15 min with gentle shaking. Then the strips were rinsed in the freshly made equilibration buffer-2 (50 mM Tris − HCl, pH 8.8, containing 6 M urea, 30% glycerol, 2% SDS, trace amount of bromophenol blue and 45 mg/ml iodoacetamide) for 10 min with gentle shaking. Next the IPG strips were rinsed in the SDS-gel running buffer before transferring into 12% SDS-gels. The SDS-gels were run at 15 °C until the dye front running out of the gels.

Gel images were scanned immediately following the SDS-PAGE using Typhoon TRIO (GE Healthcare). The scanned images were then analyzed by Image Quant software (version 6.0, GE Healthcare), followed by in-gel analysis using DeCyder software (version 6.5, GE Healthcare). The fold change of the protein expression levels was obtained from in-gel DeCyder analysis.

The spots of interest were picked up by Ettan Spot Picker (Amersham BioSciences) based on the in-gel analysis and spot picking design by DeCyder software. The gel spots were washed a few times then digested in-gel with modified porcine trypsin protease (Trypsin Gold, Promega). The digested tryptic peptides were desalted by Zip-tip C18 (Millipore). Peptides were eluted from the Zip-tip with 0.5 μl of matrix solution (cyano-4-hydroxycinnamic acid (5 mg/ml in 50% acetonitrile, 0.1% trifluoroacetic acid, 25 mM ammonium bicarbonate) and spotted on the AB SCIEX MALDI plate (Opti-TOF™ 384 Well Insert).

For protein identification, the resulting peptide mass and the associated fragmentation spectra were submitted to GPS Explorer workstation equipped with MASCOT search engine (Matrix science) to search Swiss-Prot database. Searches were performed without constraining protein molecular weight or isoelectric point, with variable carbamidomethylation of cysteine and oxidation of methionine residues, and with one missed cleavage also allowed in the search parameters. Candidates with either protein score C.I.% or Ion C.I.% greater than 95 were considered significant.

2.8. Quantitative Western Blot Analysis

Pellets were lysed by passage through a 27-gauge needle in RIPA buffer (Sigma) with protease and phosphatase inhibitors (Thermo Scientific Pierce). The lysates were cleared by centrifugation and concentrated. Protein concentration was measured using the Pierce Rapid Gold BCA Protein Assay kit. For each sample, 26 μl of sample diluted in water was mixed with 4.0 μl Bolt Reducing agent (Novex by Life technologies) and 10 μl Bolt LDS sample buffer (Novex by Life Technologies) and heated in a thermal cycler at 70 °C for 10 min.

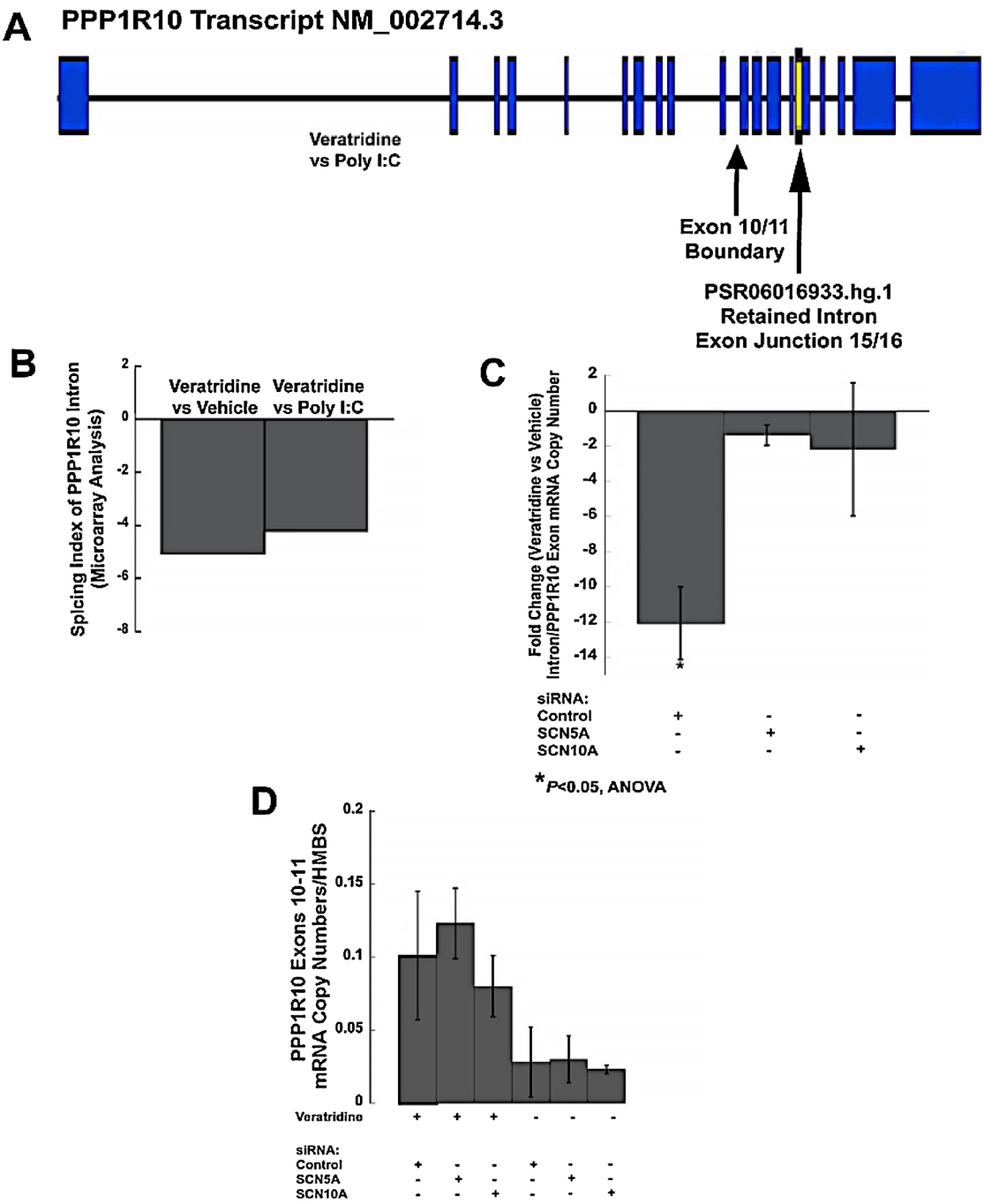

Fig. 4. Channel-dependent splicing of a retained intron in *PPP1R10* transcripts. (A) A diagram of *PPP1R10* transcripts shows the region of the retained intron identified by microarray analysis (between exons 15 and 16; also see Tables 1 and 2) and a common exon target site that spans two exons (exons 10 and 11). (B) Relative change in expression of the retained *PPP1R10* intron with veratridine treatment as determined by Affymetrix microarray analysis (Table 1). The relative expression of this intron segment is normalized to the global gene expression for *PPP1R10*. Similar results were observed with veratrdine treatment as compared to either vehicle (DMSO) or cytosolic poly I:C. Statistical analysis of these data are shown in Table 1. (C) Using quantitative real time PCR, the relative expression of transcripts containing the retained intron of *PPP1R10* was compared to expression of the upstream exon segments (exons 10/11). Pharmacological activation of human monocyte-derived macrophages (MDM) by veratridine (versus vehicle control DMSO) led to a marked decrease in the relative expression of the intron segment in the control siRNA condition. This change in the relative expression of the intron segment to the exon segments is similar to or greater than that observed in the microarray experiments (B). Knockdown of either *SCN5A* or *SCN10A* markedly diminished the response. Following treatment of MDM with veratridine, the fold change in relative intron copy number (primer targeted to intron between exons 15 and 16) as compared to an upstream exon junction (primer that spanned exons 10 and 11) was.

-12.07 $\pm$ 2.05 copies for the control siRNA condition (scr, scrambled siRNA), -1.39 $\pm$ 0.57 with *SCN5A* knockdown, and -2.21 $\pm$ 3.77 with *SCN10A* knockdown (n = 9, $P < 0.05$, scr versus *SCN5A* and *SCN10A*, *ANOVA*). (D) Although there was a modest increase in overall exon 10/11 expression in response to veratridine treatment in all siRNA conditions, the relative expression was not significant between siRNA conditions.

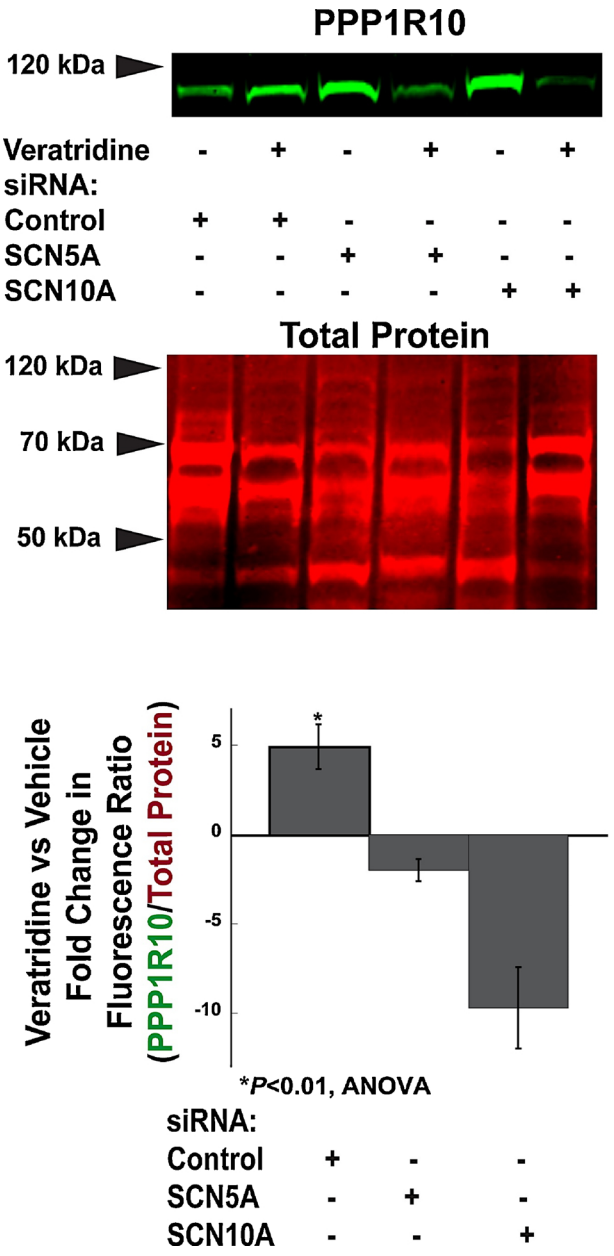

Fig. 5. Veratridine activation of human MDM increases protein expression of *PPP1R10* that is dependent on SCN5A and SCN10 A expression. Veratridine (100 μM for 2 h in serum-free media) treatment of human MDM led to increased protein expression of *PPP1R10* as determined by Western blot analysis (upper blot, green). For these experiments, quantitative Western blot analysis was performed using the Licor infrared detection system. Signal intensity was normalized to total protein staining (REVERT protein stain) because of known changes in expression of housekeeping genes in macrophages that are dependent on cell phenotype and activation conditions. Blots were imaged on a Licor Odyssey CLx system using near infrared fluorescence. *PPP1R10* staining is shown in green (800 nm), and total protein staining is shown in red (700 nm). One representative blot is shown. Fold change was normalized across multiple donors and calculated as the change in fluorescence ratio of antibody stain at 800 nm (green) to total protein stain at 700 nm (red) in the two treatment conditions (Fluorescence ratio with veratridine/fluoresence ratio with vehicle). Quantitative analysis was performed on four separate blots from independent experiments and donors (ImageStudioLite, Licor). The relative increase in PPP1R10 expression normalized to total protein was 4.90 ± 1.24 RFU's for the control siRNA condition, -2.01 ± 0.61 RFU's with SCN5A knockdown, and -9.72 ± 2.26 RFU's with SCN10 A knockdown (n = 4, $P < 0.01$, scr control versus SCN5A and SCN10A, *ANOVA*) (For interpretation of the references to colour in this figure legend, the reader is referred to the web version of this article).

Samples were run on Bolt 4–12% Bis-Tris Plus gels (Invitrogen) at 100v for 75 min. Gels where then soaked in 20% Ethanol for 5 min and transferred to 0.2 μm nitrocellulose membrane, iBlot 2 NC stacks, using the iBlot 2 system (Invitrogen) P0 preset (20v 1 min, 23v 4 min, 25v 2 min). Membranes were immediately stained using REVERT total protein stain kit (Licor) and imaged using Odyssey CLx at 700 nm. Membranes were blocked in PBS based Odyssey blocking buffer (Licor) overnight at 4 °C. The membranes were then incubated with antibodies using the iBind system (Life technologies) and the iBind FD solution kit (Novex by Life technologies) for 2.5 h. IRDye 800CW secondary antibodies (LI − COR) were used at 1:4000. Membranes were then washed with water and imaged using near infrared fluorescence on the Odyssey CLx at 800 nm. The images from the total protein stain at 700 nm (REVERT) and antibody stain at 800 nm were then analyzed by Image Studio (Licor). Fluorescence intensity at 800 nm (antibody stain) was normalized to that at 700 nm (total protein). Normalization to total protein was utilized because of increased accuracy of quantitative measurements and changes in macrophage expression of commonly utilized housekeeping genes with pharmacological treatments.

2.9. Statistical analysis

Data were analyzed as indicated using NetAffx, ImageJ, Axiovision, and Kaleidagraph (*t-test* and *ANOVA*).

3. Results

3.1. Channel activation regulates splicing of retained introns

Human Transcriptome Arrays (HTA 2.0, Affymetrix) were utilized to analyze alternative splicing in primary, human monocyte-derived macrophages (MDM). Data generated from these arrays measure expression levels of exon junctions in addition to exons and retained introns. This array approach has a higher degree of reliability as compared to older approaches and has been verified as an alternative approach to RNAseq to identify splice variants (Seok et al., 2015; Romero et al., 2016). This analysis reveals changes in specific exon and intron regions relative to the global expression of that gene.

Expression analysis of MDM revealed that pharmacological activation with veratridine (100 μM for 2 h in HBSS) leads to loss of retained introns in some transcripts (GEO NCBI submission, GSE112501, http://www.ncbi.nlm.nih.gov/geo/query/acc.cgi?acc=GSE112501). This finding was observed in the veratridine-treated condition versus vehicle (DMSO) and versus cytosolic poly I:C treatment. The most marked effect was observed for *PPP1R10* (protein phosphatase 1 regulatory subunit 10, also called PNUTS), a regulator of protein phosphatase 1 (*PP1*) and mediator of DNA repair (Kim et al., 2003; Landsverk et al., 2010). The retained intron is located between exons 15 and 16 of *PPP1R10* transcripts, and veratridine treatment reduces the relative expression of this sequence (Table 1). This effect was not due to a global increase in transcription of the gene because no differences were observed in the sum total of all *PPP1R10* transcripts or in the expression of specific exons. Gene-wide changes in *PPP1R10* transcripts and expression of representative exons (exons 10 and 11) are shown in Table 2. These results revealed a channel-activated mechanism of RNA splicing in human MDM that can occur independently of cytoplasmic poly I:C signaling.

3.2. Human macrophage SCN10A is also a novel macrophage splice variant

Since cytosolic poly I:C treatment did not regulate splicing of these transcripts, the results suggested that dsRNA activation of *SCN5A* or other cytoplasmic sensors was not sufficient to mediate the response. A second signal or an alternative ligand may be required to fully activate macrophage *SCN5A* to mimic the response observed with veratridine.

Alternatively, a different intracellular sodium channel could

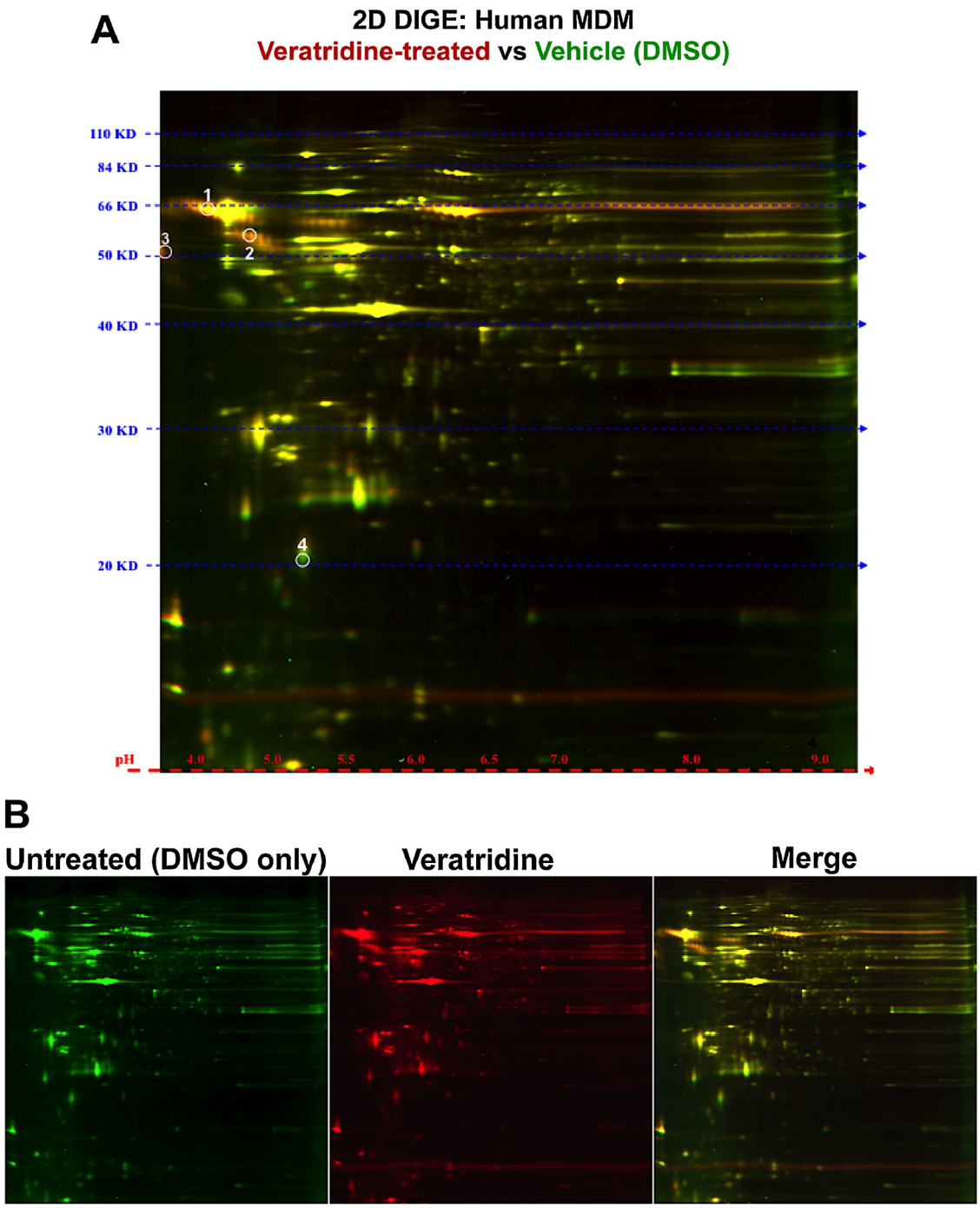

Fig. 6. Proteomic analysis of differentially expressed proteins in human macrophages. (A) 2D DIGE analysis demonstrated differential protein expression following veratridine treatment of MDM. Four of these regions yielded protein identification by mass spectroscopy with high confidence (Table 4). Spot #2 was identified as *EFTUD2*, a splicing factor with GTPase activity. (B) Source images for analysis of differential protein expression. The control condition (untreated; DMSO vehicle only) is shown on the left in green. The veratridine-treated condition (middle image) is in the red channel. The merged image is shown on the right. (For interpretation of the references to colour in this figure legend, the reader is referred to the web version of this article).

regulate intronic splicing in response to pharmacological activation, either independently of *SCN5A* or as a required second signal. Our next goal was to discover other voltage-gated sodium channel transcripts that are expressed in human macrophages and contain an exon deletion similar to the variant *SCN5A* channel (Rahgozar et al., 2013). As compared to transcripts from human heart and dorsal root ganglia (DRG), splicing analysis revealed expression of *SCN10A* transcripts in human MDM that contain a similar exon deletion that encodes for the extracellular selectivity filter (Table 3). Both exon 23 in *SCN10A* and exon 24 in *SCN5A* encode a short amino acid sequence within the extracellular selectivity filter of the channels (Fig. 1AB).

These results were subsequently confirmed by qPCR analysis (Fig. 1C). For human DRG samples, *SCN10A* mRNA copies/(*HMBS* copy number) were 2.91 $\pm$ 0.11 and 8.36 $\pm$ 0.42, respectively for a common exon span (exon 15 and 16) and exon 23. For human MDM, SCN10 A mRNA copies/(*HMBS* copy number x10^{-2}) were 3.08 $\pm$ 0.16 for the common exon span but were not detected (ND) for exon 23. *HMBS* (hydroxymethylbilane synthase) was utilized as the housekeeping gene for normalization between samples (n = 4 for each condition).

Table 4
Nano-LC MS/MS analysis of 2D DIGE of MDM (veratridine treated versus vehicle).

Spot no.	Fold Change	Protein ID	Peptide Count	Total Ion Score	Total Ion C.I. %
1	2.5	AHSG	5	61	100
2	2.4	EFTUD2	8	40	98
3	2.1	Rab-37	8	27	64
4	−2.2	GM2A	4	57	100

Peaks from liquid chromatography were analyzed by mass spectroscopy. The ion score is based on probability of a peptide match with known database proteins. The total ion score is a sum of the scores for all peptide fragments that match a specific protein. The total ion confidence interval (C.I.) is a normalized probability.

3.3. The SCN10A splice variant localizes to cytoplasmic and nuclear vesicles in human macrophages

Immunofluorescence staining of human MDM for *SCN10A* revealed an intracellular localization that demonstrated a vesicular appearance, similar to the staining pattern previously obtained for human macrophage *SCN5A* (Carrithers et al., 2007). This staining pattern suggested a predominant localization to cytoplasmic endosomes. However, deconvolution microscopy analysis also demonstrated localization of *SCN10A* to vesicles within the nucleus and showed a similar level of nuclear expression as compared to *PRP8*, a nuclear protein that is a component of the spliceosome (Fig. 2). Localization was not observed in the nucleolus as demonstrated by the absence of DAPI staining (Fig. 2, white arrows).

Since some of these *SCN10A*-positive vesicles may be associated with the nuclear envelope membrane, a marker for the nuclear envelope, Lamin A, was utilized to assess for co-localization. Staining demonstrated the localization of a small number *SCN10 A* vesicles that co-localize with Lamin A, a marker of the nuclear envelope membrane (white arrows, Fig. 3). However, the majority of perinuclear and intranuclear *SCN10A*-positive vesicles do not co-localize with Lamin A. These results suggested that some *SCN10A*-positive vesicles are intranuclear as has been observed for nucleoplasmic calcium storage vesicles (Yoo et al., 2014).

3.4. Expression of human macrophage SCN5A and SCN10A is required for channel activation dependent splicing of the retained intron in PPP1R10 transcripts

Since cytosolic poly I:C treatment did not regulate splicing of PPP1R10 transcripts, the results suggested that dsRNA activation of SCN5A or other cytoplasmic sensors was not sufficient to mediate the response. Therefore, we hypothesized that human macrophage SCN10A regulates this pathway. The next goal was to confirm intronic splicing in response to veratridine activation by quantitative real time PCR in human MDM and determine if siRNA-mediated knockdown of either SCN5A or SCN10A inhibited this response (Fig. 4A).

In the microarray experiments discussed above, treatment of MDM with veratridine reduced the expression of a *PPP1R10* intron segment located between exons 15 and 16 by approximately 5-fold as compared to the vehicle treatment condition (Table 1; Fig. 4B). There was no statistically relevant change in gene-fold level transcription or in the representative exon segments 10 and 11.

To confirm the array results and to analyze the effects of channel knockdown, the relative fold change in the expression of the retained intron (primer targeted to intron between exons 15 and 16) was normalized to the expression of the representative upstream exons (primer that spanned exons 10 and 11). Although there was a modest increase in overall exon 10/11 expression in all conditions (veratridine treatment versus vehicle), this relative increase was not significant between conditions (Fig. 4D). However, the fold change in intron copy number in response to veratridine treatment (normalized to exon expression) was -12.07 $\pm$ 2.05 copies for the control siRNA condition (scr, scrambled siRNA), -1.39 $\pm$ 0.57 with *SCN5A* knockdown, and -2.21 $\pm$ 3.77 with *SCN10A* knockdown (n = 9 from multiple donors, $P < 0.05$, scr versus *SCN5A* and *SCN10A*, *ANOVA*). This 12-fold decrease in relative intron expression was greater than the 5-fold change observed in the micorarray splicing analysis (Table 1; Fig. 4C). These results suggested that the relative change in expression of the retained intron was due to splicing rather than an increase in new transcripts that lacked the intron. In addition, co-expression of human macrophage *SCN5A* and *SCN10A* was necessary to mediate this response.

3.5. Channel activation increases PPP1R10 protein expression

The next goal was to analyze the effects on intron splicing on *PPP1R10* protein expression. For these experiments, quantitative Western blot analysis was performed using the LiCor infrared detection system. Signal intensity for antibody staining (800 nm channel) was normalized to total protein staining (700 nm channel) because of known changes in expression of housekeeping genes in macrophages that are dependent on cell phenotype and activation conditions. Western blot analysis demonstrated a relative increase in *PPP1R10* protein levels following veratridine activation (Fig. 5). Knockdown of either *SCN5A* or *SCN10A* led to the converse response with a marked decrease following channel activation. The relative increase in *PPP1R10* expression normalized to total protein (fold change in fluorescence ratio of antibody stain at 800 nm to total protein stain at 700 nm) was 4.90 $\pm$ 1.24 RFU's (relative fluorescence units) for the control siRNA condition, -2.01 $\pm$ 0.61 RFU's with *SCN5A* knockdown, and -9.72 $\pm$ 2.26 RFU's with *SCN10A* knockdown (n = 5, $P < 0.01$, scr control versus *SCN5A* and *SCN10A*, *ANOVA*). These results suggested that human macrophage *SCN5A* and *SCN10A* synergistically regulate RNA processing and translation to increase expression of *PPP1R10*.

3.6. Channel activation increases expression of EFTUD2, a splicing factor with GTPase activity

The next goal was to identify additional proteins that are regulated by channel activation and discover possible mechanisms that could regulate channel activity-dependent RNA splicing. Differential protein expression between veratridine-treated and untreated MDM were analyzed by 2D DIGE followed by mass spectroscopy (Fig. 6, Table 4). Several proteins demonstrated increased expression in response to channel activation. One of these, *EFTUD2* (Elongation Factor Tu GTP Binding Domain Containing 2), regulates RNA splicing (Fabrizio et al., 1997).

These results were confirmed by Western blot analysis and immunofluorescence staining (Fig. 7A). By quantitative Western blot analysis, the relative increase in *EFTUD2* expression normalized to total protein (ratio of fluorescence intensity at 800 nm to 700 nm) was 2.07 $\pm$ 0.36 RFU's for the control siRNA condition, -2.68 $\pm$ 1.33 RFU's with *SCN5A* knockdown, and -2.75 $\pm$ 0.78 RFU's with *SCN10A* knockdown (n = 4, $P < 0.05$, scr control versus *SCN5A* and *SCN10A*, *ANOVA*). Microarray analysis (GEO NCBI submission, GSE112501, http://www.ncbi.nlm.nih.gov/geo/query/acc.cgi?acc = GSE112501, data set used in Tables 1 and 2) did not show an increase in global RNA expression or in alternative splicing of *EFTUD2*. These results suggested that channel-dependent regulation of *EFTUD2* protein expression occurred at the level of translation rather than RNA splicing.

Knockdown of *EFTUD2* in human MDM also inhibited splicing of the retained intron in *PPP1R10* transcripts in response to pharmacological activation with veratridine (Fig. 7B). As shown in Fig. 4, pharmacological activation of MDM by veratridine (versus vehicle control DMSO) led to a marked decrease in the relative expression of the intron

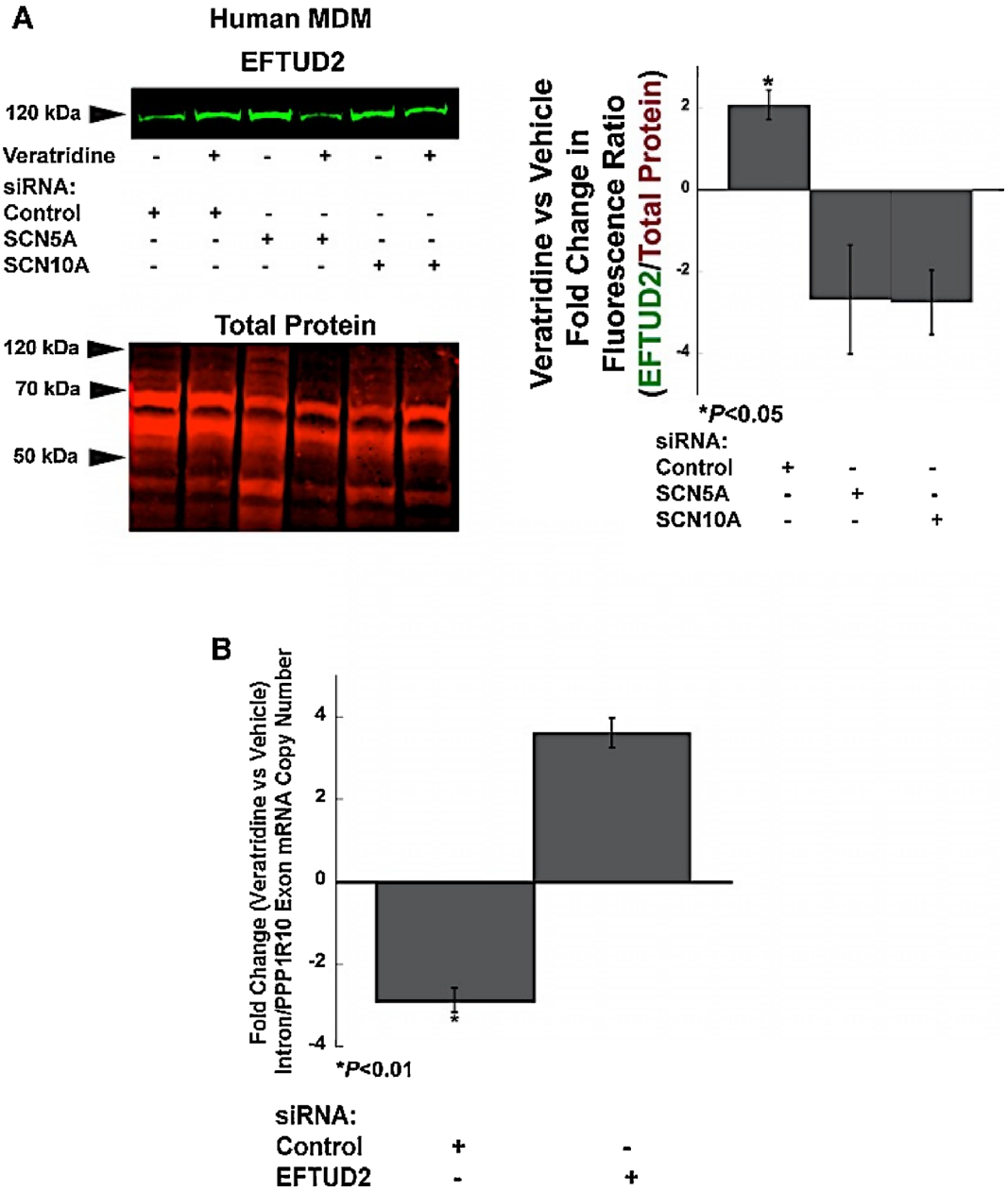

Fig. 7. Channel activation increases expression of *EFTUD2*, and EFTUD2 knockdown prevents channel-dependent decrease in the retained *PPP1R10* intron. (A) Veratridine (100 μM for 2 h in serum-free media) treatment of human MDM led to increased protein expression of *EFTUD2* as determined by Western blot analysis (upper blot, green). This response was not observed following siRNA-mediated knockdown of either *SCN5A* or *SCN10A*. Total protein staining and imaging were performed as described in Fig. 5. The relative increase in *EFTUD2* expression normalized to total protein was 2.07 ± 0.36 RFU's for the control siRNA condition, -2.68 ± 1.33 RFU's with *SCN5A* knockdown, and -2.75 ± 0.78 RFU's with *SCN10A* knockdown (n = 4, $P < 0.05$, scr control versus *SCN5A* and *SCN10A*, *ANOVA*). (B) Quantitative real time PCR was performed as described in Fig. 4. As described for those experiments, the relative expression of transcripts containing the retained intron of *PPP1R10* was compared to expression of the upstream exon segments (exons 10/11). Pharmacological activation of MDM by veratridine (versus vehicle control DMSO) led to a marked decrease in the relative expression of the intron segment in the control siRNA condition, but not in the *EFTUD2* knockdown condition. The fold change in the control siRNA condition was -2.87 ± 0.30 copies versus 3.62 ± 0.37 for the *EFTUD2* knockdown condition (n = 4, $P < 0.01$) (For interpretation of the references to colour in this figure legend, the reader is referred to the web version of this article).

segment in the control siRNA condition. (The donors utilized for these experiments were unique as compared to those used in Fig. 4.) However, this response was not observed in the *EFTUD2* knockdown condition. The fold change in the control siRNA condition was -2.87 ± 0.30 copies versus 3.62 ± 0.37 for the *EFTUD2* knockdown condition (n = 4, $P < 0.01$). These results suggested that increased protein expression of *EFTUD2* is necessary for channel-dependent RNA processing in human MDM.

3.7. Knockdown of SCN5A or SCN10A expression in human macrophages increases the severity of a DNA damage response

Because *PPP1R10* is a known mediator of DNA repair, we reasoned that inhibition of channel-mediated signaling would limit DNA repair during a DNA damage response. The next goal was to assess the effect of *SCN5A* and *SCN10A* expression in human MDM during chemical induction of dsDNA breaks. The severity of this response can be detected by nuclear staining for γH2AX, a marker of dsDNA breaks.

Prior work from another laboratory demonstrated that mouse

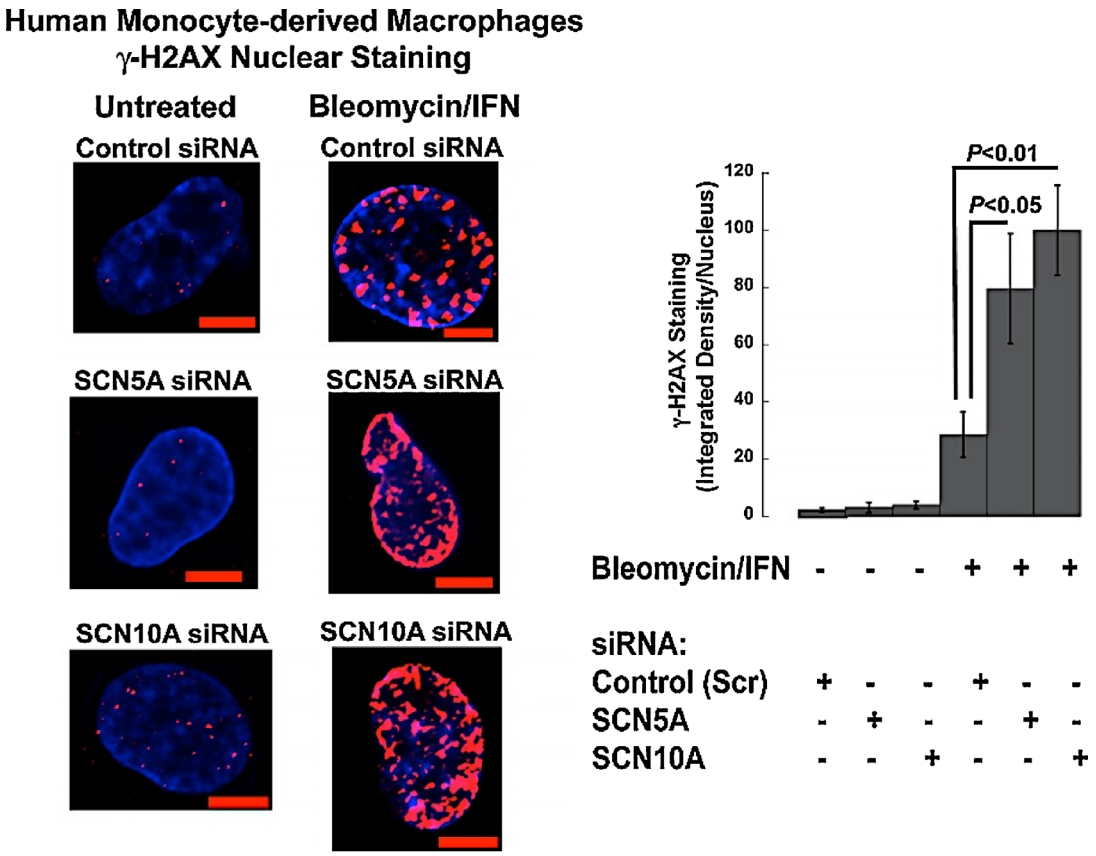

Fig. 8. Knockdown of *SCN5A* or *SCN10A* expression in human macrophages increases the severity of a DNA damage response as determined by γH2AX nuclear staining. Human monocyte-derived macrophages were treated with bleomycin (1 μg/ml) and type I interferon (human IFN-alpha A/D; 100 U/ml) for 6 h to induce dsDNA breaks. Cells were stained for γH2AX (red), a marker of dsDNA breaks, and subsequently counterstained with the nuclear marker DAPI (blue). Images were acquired and processed by deconvolution, fluorescence microscopy, and the density of γH2AX per nucleus was determined by ImageJ. No differences in nuclear staining density were obseved in the control, untreated condition. However, knockdown of either *SCN5A* or *SCN10A* resulted in an increase in staining density for γH2AX as compared to the control siRNA condition. Data are shown in Table 5 (For interpretation of the references to colour in this figure legend, the reader is referred to the web version of this article).

Table 5
Quantitiative analysis of γH2AX nuclear staining of human monocyte-derived macrophages (MDM) in the presence and absence of bleomycin/IFN treatment.

siRNA	Bleomycin/IFN	Integrated Density/Nucleus (RFU's)	Microscopic Fields (n)
Scrambled	–	2.21 ± 0.82	12
SCN5A	–	3.06 ± 1.85	15
SCN10A	–	3.94 ± 1.37	9
Scrambled	+	28.56 ± 7.85	7
SCN5A	+	79.57 ± 19.28*	11
SCN10A	+	100.01 ± 15.77**	11

MDM were treated with bleomycin (1 μg/ml) and human IFN-alpha A/D (100 U/ml) for 6 h.
* $P < 0.05$ versus Scrambled Belomycin/IFN-treated.
** $P < 0.01$ versus Scrambled Belomycin/IFN-treated.

macrophages are relatively resistant to chemical induction of dsDNA breaks and require co-treatment with bleomycin, an inducer of DNA strand breaks, and type I interferon (human IFN-alpha A/D; 100 U/ml) (Morales et al., 2017). In human MDM, this treatment also induced a robust damage response as demonstrated by an increase in nuclear staining for γH2AX, a marker of dsDNA breaks. siRNA-mediated knockdown of either *SCN5A* or *SCN10A* markedly increased the severity of the response (micrographs shown in Fig. 8; data analysis in Table 5). These results suggested a functional link between channel-dependent regulation of *PPP1R10* expression and DNA repair.

The effects of channel knockdown on the formation of dsDNA breaks was analyzed further by staining for TP53BP1 (tumor protein p53 binding protein 1). This DNA repair protein is recruited to regions of dsDNA breaks and promotes non-homologous end-joining (NHEJ) pathways (Dimitrova et al., 2008). This step in the DNA damage response occurs downstream of phosphorylation of H2AX. Treatment of human MDM with bleomycin and type I interferon increased nuclear staining for TP53BP1 (Fig. 9, Table 6) in all conditions. Knockdown of *SCN5A* led to an increase in TP53BP1 nuclear staining as compared to the scrambled, siRNA condition. Knockdown of *SCN10A* had a more marked effect, and the increase in staining of nuclear TP53BP1 foci was greater than that in all conditions, including the *SCN5A* condition. These results suggested that expression of both channels reduce DNA damage induced by bleomycin and Type 1 interferon. It also suggested that human macrophage *SCN10A* may regulate multiple pathways that enhance DNA repair.

4. Discussion

We here demonstrate a potential mechanism to link innate immune signaling in human macrophages to DNA repair. The proposed mechanism is that simultaneous activation of *SCN5A* and *SCN10A* increases expression of *PPP1R10* protein expression through cleavage of a retained intron in *PPP1R10* transcripts. This increase in *PPP1R10* protein expression is dependent on expression of the spliceosome protein, *EFTUD2*. The prediction is that this channel-dependent increase in *PPP1R10* expression enhances DNA repair to prevent amplification of inflammatory injury.

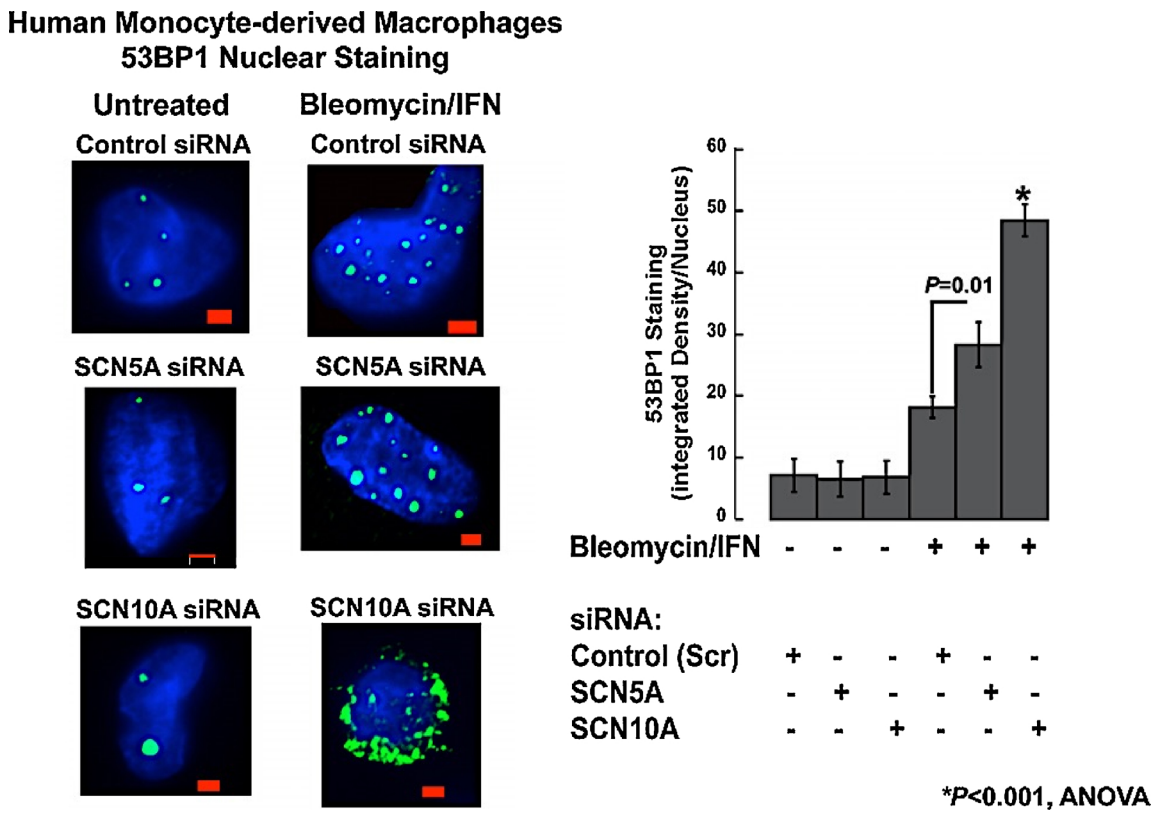

Fig. 9. Knockdown of *SCN5A* or *SCN10A* expression in human macrophages increases the severity of a DNA damage response as determined by 53BP1 staining. Human monocyte-derived macrophages were treated with bleomycin (1 μg/ml) and type I interferon (human IFN-alpha A/D; 100 U/ml) for 6 h to induce dsDNA breaks. Cells were stained for 53BP1 (green), a marker of dsDNA breaks, and subsequently counterstained with the nuclear marker DAPI (blue). Images were acquired and processed by deconvolution, fluorescence microscopy, and the density of 53BP1 per nucleus was determined by ImageJ. No differences in nuclear staining density were obseved in the control, untreated condition. However, knockdown of either *SCN5A* or *SCN10 A* resulted in an increase in staining density for 53BP1 as compared to the control siRNA condition. Data are shown in Table 6 (For interpretation of the references to colour in this figure legend, the reader is referred to the web version of this article).

Table 6
Quantitiative analysis of TP53BP1 nuclear staining of human monocyte-derived macrophages (MDM) in the presence and absence of bleomycin/IFN treatment.

siRNA	Bleomycin/IFN	Integrated Density/Nucleus (RFU's)	Microscopic Fields (n)
Scrambled	–	7.11 ± 2.66	14
SCN5A	–	6.55 ± 2.88	14
SCN10A	–	6.80 ± 2.68	14
Scrambled	+	18.17 ± 1.76	48
SCN5A	+	28.34 ± 3.64*	42
SCN10A	+	48.52 ± 2.56**	44

MDM were treated with bleomycin (1 μg/ml) and human IFN-alpha A/D (100 U/ml) for 6 h.

* $P = 0.01$ versus Scrambled Belomycin/IFN-treated.

** $P < 0.001$, ANOVA, versus all conditions.

As part of this study, a novel intracellular splice variant of *SCN10 A* was identified. Both *SCN5A* and *SCN10A* splice variants in human macrophages contain a deletion in a highly homologous exon that encodes the extracellular selectivity filter and a portion of the channel pore (Rahgozar et al., 2013). This deletion alters the ion selectivity of the channels so that they flux other monovalent cations such as potassium and cesium (Jones et al., 2014). Therefore, these channels function as cation channels rather than classic voltage-gated sodium channels. However, they retain voltage dependence and respond to pharmacological agents such as channel activators and inhibitors.

In these experiments, we utilized the sodium channel agonist, veratridine, to activate intracellular channels. This approach was previously utilized to identify a novel pattern recognition pathway initiated by dsRNA recognition by human macrophage *SCN5A* (Jones et al., 2014). In those experiments, veratridine and cytosolic poly I:C were shown to activate an *SCN5A*-regulated transcriptional pathway that increases synthesis of Type I interferons. Here we utilized pharmacological activation to identify *SCN5A*-dependent and independent pathways. The pathway required for endogenous activation of *SCN10A* is not known but may occur through activation by a cytosolic ligand or by voltage-dependence alone.

Simultaneous activation of macrophage variants *SCN5A* and *SCN10A* regulate selective RNA processing as determined by our RNA expression analysis. We here focused on *PPP1R10* because of the high statistical confidence (Table 1) and its potential role in regulating innate immune signaling in macrophages. *PPP1R10* is a regulatory subunit of protein phosphatase (PP1) (Kim et al., 2003) and prevents DNA damage during cell injury (Landsverk et al., 2010). Its role in DNA repair provides a rationale to link its relative expression to modulation of innate immune signaling.

Splicing of retained introns provides an additional layer of regulation for protein synthesis. Our data suggest that channel-dependent splicing of a retained intron in *PPP1R10* transcripts is due in part to increased expression of *EFTUD2*, a splicing factor with GTPase activity (Fig. 9) (Fabrizio et al., 1997). We speculate that the relative increase in *PPP1R10* protein expression is due in part to relatively low baseline expression because of the intron retention (Fig. 4). Channel activation permits release from this inhibitory mechanism to increase selective and efficient RNA translation. However, additional mechanisms of channel-dependent regulation of protein synthesis likely exist because a similar pattern of increased protein expression was observed with

EFTUD2 (Fig. 6). Based on our microarray data, this increase in *EFTUD2* protein expression was not associated with any changes in RNA expression or intron retention. Based on our prior work, these mechanisms may be calcium or GTPase-dependent (Carrithers et al., 2011). Channel-dependent regulation of intron splicing may occur through a non-canonical pathway in the cytoplasm or within the nucleus as suggested by the presence of nucleoplasmic *SCN10A*-positive vesicles. These intranuclear vesicles may regulate ionic flux from nuclear calcium stores (Yoo et al., 2014).

Knockdown of *SCN5A* or *SCN10A* expression also increased the severity of DNA damage induced by treatment with bleomycin and Type 1 interferon. These data support the mechanistic importance of channel-dependent regulation of *PPP1R10* protein expression. The proposed model is that endogenous injury of human macrophages increases *SCN5A* and *SCN10A* channel activity. Channel activation leads to cleavage of a retained intron in *PPP1R10* transcripts through an *EFTUD2*-dependent mechanism. This novel mechanism links innate immune signaling to RNA processing.

The working hypothesis is that this mechanism mediates an anti-inflammatory response to prevent injury initiated by cytoplasmic DNA sensors such as cGAS (cyclic GMP-AMP synthase) (Ablasser et al., 2013). Prior work from other laboratories has shown that DNA damage and subsequent release of dsDNA into the cytoplasm activate cGAS and the downstream signaling molecule STING (stimulator of interferon genes) (Mackenzie et al., 2017). This endogenous pathway of innate immune activation occurs in the absence of infection and leads to cellular sensescence (Yang et al., 2017). It is proposed that the channel-dependent increase in protein expression of the DNA repair protein *PPP1R10* limits injury initiated by endogenous DNA damage.

The endogenous mechanisms that simultaneously activate macrophage *SCN5A* and *SCN10A* to initate signaling in this DNA repair pathway are unclear. It could occur through at least two independent mechanisms: ligand-gated channel activation and voltage-dependent activation. This laboratory previously demonstrated that cytosolic dsRNA activates human macrophage *SCN5A* (Jones et al., 2014). Endogenous dsRNA's are present in all cells, and their concentration increases during immune stimulation (Blango and Bass, 2016). Unpublished work suggests that dsRNA is not sufficient to activate SCN10 A. However, prior work from another laboratory suggested that GTP increases neuronal *SCN10A* currents (Saab et al., 2003), and this nucleotide or related molecules and metabolites could activate the channel in human macrophages. This observation is particularly relevant to innate immune signaling in macrophages of the cytosolic cGAS/STING pattern recognition pathway for dsDNA. Recognition of dsDNA by cGAS catalyzes the synthesis of cGAMP from GTP and ATP (Nakad and Schumacher, 2016). Additional work is required to assess which nucleotides most efficiently activate human macrophage *SCN10A*. This model suggests a two signal mechanism that requires the simultaneous presence of cytosolic dsRNA to activate *SCN5A* and a nucleotide metabolite to activate *SCN10A*.

The alternative mechanism is that the channels are activated solely through voltage dependence. Increases in extracellular potassium levels are a particularly relevant danger signal in the central nervous system because of the rapid changes that can occur with impaired potassium buffering due to cell injury or death (Kofuji and Newman, 2004). Voltage-dependent activation of channels can occur in regions of cellular injury through increases in extracellular potassium and subsequent membrane depolarization. These increases in extracellular potassium are due to release of intracellular potassium by sick and dying cells.

5. Conclusions

- A novel splice variant of human *SCN10A* is expressed in human macrophages and contains a similar exon deletion to that previously identified in human macrophage *SCN5A*.
- Pharmacological activation of human macrophage *SCN5A* and *SCN10A* leads to a decrease in expression of a retained intron in transcripts of *PPP1R10*, a protein that regulates DNA repair, and an increase in *PPP1R10* protein expression.
- Pharmacological activation of human macrophage *SCN5A* and *SCN10A* is also associated with an increase in *EFTUD2*, a regulator of RNA splicing that is necessary for channel-dependent regulation of intron splicing in *PPP1R10* transcripts.
- As predicted by the association of increases in *PPP1R10* expression with channel activation, knockdown of either *SCN5A* or *SCN10 A* in human macrophages increases the severity of dsDNA breaks induced by bleomycin and Type I interferon.
- A novel mechanism of protective innate immune signaling is proposed whereby activation of intracellular sodium channels regulates intron retention and protein expression of *PPP1R10* to prevent inflammatory injury initiated by DNA damage.

Conflict of interest

The authors declare that have no conflicts of interest with the contents of this article.

Acknowledgements

The authors acknowledge the technical assistance of Hongjin Huang at Applied Biomics (Hayward, Ca.) for fluorescent 2 D-DIGE, and mass spectroscopy analysis and Dr. Wayne Davis at the University of Wisconsin Biotechnology facility for RNA probe labeling, microarray hybridization and slide scanning.

This work was supported by a Merit Award from the BLR&D service of the U.S. Department of Veterans Affairs, BX000467-05. The content is solely the responsibility of the authors and does not represent the official views of the U.S. Department of Veterans Affairs.

References

Ablasser, A., Goldeck, M., Cavlar, T., Deimling, T., Witte, G., Rohl, I., Hopfner, K.P., Ludwig, J., Hornung, V., 2013. cGAS produces a 2'-5'-linked cyclic dinucleotide second messenger that activates STING. Nature 498 (7454), 380–384. https://doi.org/10.1038/nature12306. PubMed PMID: 23722158; PubMed Central PMCID: PMC4143541.

Blango, M.G., Bass, B.L., 2016. Identification of the long, edited dsRNAome of LPS-stimulated immune cells. Genome Res. 26 (6), 852–862. https://doi.org/10.1101/gr.203992.116. PubMed PMID: 27197207; PubMed Central PMCID: PMC4889969.

Carrithers, M.D., Dib-Hajj, S., Carrithers, L.M., Tokmoulina, G., Pypaert, M., Jonas, E.A., Waxman, S.G., 2007. Expression of the voltage-gated sodium channel NaV1.5 in the macrophage late endosome regulates endosomal acidification. J. Immunol. 178 (12), 7822–7832 Epub 2007/06/06. doi: 178/12/7822 [pii]. PubMed PMID: 17548620.

Carrithers, L.M., Hulseberg, P., Sandor, M., Carrithers, M.D., 2011. The human macrophage sodium channel NaV1.5 regulates mycobacteria processing through organelle polarization and localized calcium oscillations. FEMS Immunol. Med. Microbiol. 63 (3), 319–327. https://doi.org/10.1111/j.1574-695X.2011.00853.x. Epub 2011/11/19 PubMed PMID: 22092558.

Dimitrova, N., Chen, Y.C., Spector, D.L., de Lange, T., 2008. 53BP1 promotes non-homologous end joining of telomeres by increasing chromatin mobility. Nature 456 (7221), 524–528. https://doi.org/10.1038/nature07433. PubMed PMID: 18931659; PubMed Central PMCID: PMC2613650.

Fabrizio, P., Laggerbauer, B., Lauber, J., Lane, W.S., Luhrmann, R., 1997. An evolutionarily conserved U5 snRNP-specific protein is a GTP-binding factor closely related to the ribosomal translocase EF-2. EMBO J. 16 (13), 4092–4106. https://doi.org/10.1093/emboj/16.13.4092. PubMed PMID: 9233818; PubMed Central PMCID: PMC1170032.

Ishikawa, H., Ma, Z., Barber, G.N., 2009. STING regulates intracellular DNA-mediated, type I interferon-dependent innate immunity. Nature 461 (7265), 788–792. https://doi.org/10.1038/nature08476. PubMed PMID: 19776740; PubMed Central PMCID: PMC4664154.

Jones, A., Kainz, D., Khan, F., Lee, C., Carrithers, M.D., 2014. Human macrophage SCN5A activates an innate immune signaling pathway for antiviral host defense. J. Biol. Chem. 289 (51), 35326–35340. https://doi.org/10.1074/jbc.M114.611962. PubMed PMID: 25368329; PubMed Central PMCID: PMC4271219.

Kim, Y.M., Watanabe, T., Allen, P.B., Kim, Y.M., Lee, S.J., Greengard, P., Nairn, A.C., Kwon, Y.G., 2003. PNUTS, a protein phosphatase 1 (PP1) nuclear targeting subunit. Characterization of its PP1- and RNA-binding domains and regulation by phosphorylation. J. Biol. Chem. 278 (16), 13819–13828. https://doi.org/10.1074/jbc.M209621200. PubMed PMID: 12574161.

Kofuji, P., Newman, E.A., 2004. Potassium buffering in the central nervous system.

Neuroscience 129 (4), 1045–1056. https://doi.org/10.1016/j.neuroscience.2004.06.008. PubMed PMID: 15561419; PubMed Central PMCID: PMC2322935.

Landsverk, H.B., Mora-Bermudez, F., Landsverk, O.J., Hasvold, G., Naderi, S., Bakke, O., Ellenberg, J., Collas, P., Syljuasen, R.G., Kuntziger, T., 2010. The protein phosphatase 1 regulator PNUTS is a new component of the DNA damage response. EMBO Rep. 11 (11), 868–875. https://doi.org/10.1038/embor.2010.134. PubMed PMID: 20890310; PubMed Central PMCID: PMC2966950.

Lee, C., Jones, A., Kainz, D., Khan, F., Carrithers, M.D., 2015. A sodium channel variant in Aedes aegypti as a candidate pathogen sensor for viral-associated molecular patterns. Biochem. Biophys. Res. Commun. https://doi.org/10.1016/j.bbrc.2015.06.085. PubMed PMID: 26086103.

Li, P., Du, J., Goodier, J.L., Hou, J., Kang, J., Kazazian Jr., H.H., Zhao, K., Yu, X.F., 2017. Aicardi-Goutieres syndrome protein TREX1 suppresses L1 and maintains genome integrity through exonuclease-independent ORF1p depletion. Nucleic Acids Res. 45 (8), 4619–4631. https://doi.org/10.1093/nar/gkx178. PubMed PMID: 28334850; PubMed Central PMCID: PMC5416883.

Mackenzie, K.J., Carroll, P., Martin, C.A., Murina, O., Fluteau, A., Simpson, D.J., Olova, N., Sutcliffe, H., Rainger, J.K., Leitch, A., Osborn, R.T., Wheeler, A.P., Nowotny, M., Gilbert, N., Chandra, T., Reijns, M.A.M., Jackson, A.P., 2017. cGAS surveillance of micronuclei links genome instability to innate immunity. Nature 548 (7668), 461–465. https://doi.org/10.1038/nature23449. . PubMed PMID: 28738408; PubMed Central PMCID: PMC5870830.

Morales, A.J., Carrero, J.A., Hung, P.J., Tubbs, A.T., Andrews, J.M., Edelson, B.T., Calderon, B., Innes, C.L., Paules, R.S., Payton, J.E., Sleckman, B.P., 2017. A type I IFN-dependent DNA damage response regulates the genetic program and inflammasome activation in macrophages. eLife 6https://doi.org/10.7554/eLife.24655. PubMed PMID: 28362262; PubMed Central PMCID: PMC5409825.

Nakad, R., Schumacher, B., 2016. DNA damage response and immune defense: links and mechanisms. Front. Genet. 7, 147. https://doi.org/10.3389/fgene.2016.00147. PubMed PMID: 27555866; PubMed Central PMCID: PMC4977279.

Poltorak, A., He, X., Smirnova, I., Liu, M.Y., Van Huffel, C., Du, X., Birdwell, D., Alejos, E., Silva, M., Galanos, C., Freudenberg, M., Ricciardi-Castagnoli, P., Layton, B., Beutler, B., 1998. Defective LPS signaling in C3H/HeJ and C57BL/10ScCr mice: mutations in Tlr4 gene. Science 282 (5396), 2085–2088 PubMed PMID: 9851930.

Rahgozar, K., Wright, E., Carrithers, L.M., Carrithers, M.D., 2013. Mediation of Protection and Recovery From Experimental Autoimmune Encephalomyelitis by Macrophages Expressing the Human Voltage-Gated Sodium Channel NaV1.5. J. Neuropathol. Exp. Neurol. 72 (6), 489–504. https://doi.org/10.1097/NEN.0b013e318293eb08. Epub 2013/05/10 PubMed PMID: 23656992.

Rice, G.I., Forte, G.M., Szynkiewicz, M., Chase, D.S., Aeby, A., Abdel-Hamid, M.S., Ackroyd, S., Allcock, R., Bailey, K.M., Balottin, U., Barnerias, C., Bernard, G., Bodemer, C., Botella, M.P., Cereda, C., Chandler, K.E., Dabydeen, L., Dale, R.C., De Laet, C., De Goede, C.G., Del Toro, M., Effat, L., Enamorado, N.N., Fazzi, E., Gener, B., Haldre, M., Lin, J.P., Livingston, J.H., Lourenco, C.M., Marques Jr., W., Oades, P., Peterson, P., Rasmussen, M., Roubertie, A., Schmidt, J.L., Shalev, S.A., Simon, R., Spiegel, R., Swoboda, K.J., Temtamy, S.A., Vassallo, G., Vilain, C.N., Vogt, J., Wermenbol, V., Whitehouse, W.P., Soler, D., Olivieri, I., Orcesi, S., Aglan, M.S., Zaki, M.S., Abdel-Salam, G.M., Vanderver, A., Kisand, K., Rozenberg, F., Lebon, P., Crow, Y.J., 2013. Assessment of interferon-related biomarkers in Aicardi-Goutieres syndrome associated with mutations in TREX1, RNASEH2A, RNASEH2B, RNASEH2C, SAMHD1, and ADAR: a case-control study. Lancet Neurol. 12 (12), 1159–1169. https://doi.org/10.1016/S1474-4422(13)70258-8. PubMed PMID: 24183309; PubMed Central PMCID: PMC4349523.

Romero, J.P., Muniategui, A., De Miguel, F.J., Aramburu, A., Montuenga, L., Pio, R., Rubio, A., 2016. EventPointer: an effective identification of alternative splicing events using junction arrays. BMC Genomics 17, 467. https://doi.org/10.1186/s12864-016-2816-x. PubMed PMID: 27315794; PubMed Central PMCID: PMC4912780.

Saab, C.Y., Cummins, T.R., Waxman, S.G., 2003. GTP gamma S increases Nav1.8 current in small-diameter dorsal root ganglia neurons. Exp. Brain Res. 152 (4), 415–419. https://doi.org/10.1007/s00221-003-1565-7. PubMed PMID: 12898089.

Seok, J., Xu, W., Davis, R.W., Xiao, W., 2015. RASA: robust alternative splicing analysis for human transcriptome arrays. Sci. Rep. 5, 11917. https://doi.org/10.1038/srep11917. PubMed PMID: 26145443; PubMed Central PMCID: PMC4491729.

Yang, H., Wang, H., Ren, J., Chen, Q., Chen, Z.J., 2017. cGAS is essential for cellular senescence. Proc. Natl. Acad. Sci. U. S. A. 114 (23). https://doi.org/10.1073/pnas.1705499114. E4612-E20 PubMed PMID: 28533362; PubMed Central PMCID: PMC5468617.

Yoneyama, M., Kikuchi, M., Natsukawa, T., Shinobu, N., Imaizumi, T., Miyagishi, M., Taira, K., Akira, S., Fujita, T., 2004. The RNA helicase RIG-I has an essential function in double-stranded RNA-induced innate antiviral responses. Nat. Immunol. 5 (7), 730–737. https://doi.org/10.1038/ni1087. PubMed PMID: 15208624.

Yoo, S.H., Huh, Y.H., Huh, S.K., Chu, S.Y., Kim, K.D., Hur, Y.S., 2014. Localization and projected role of phosphatidylinositol 4-kinases IIalpha and IIbeta in inositol 1,4,5-trisphosphate-sensitive nucleoplasmic Ca(2)(+) store vesicles. Nucleus 5 (4), 341–351. https://doi.org/10.4161/nucl.29776. PubMed PMID: 25482123; PubMed Central PMCID: PMC4152348.